A model of the diffuse gamma-ray emission from the central region of NGC 253

E. Domingo-Santamaría[a] and Diego F. Torres[b]
(a) Institut de Física d'Altes Energies, Edifici C-n, Campus UAB, 08193 Bellaterra, Spain
(b) Lawrence Livermore National Laboratory, 7000 East Ave. L-413, Livermore, CA 94550, USA
Presenter: E. Domingo-Santamaría (domingo@ifae.es), spa-domingo-santamaria-E-abs1-og21-oral

This paper discusses a model for the diffuse emission of gamma-rays (produced as secondaries of cosmic ray interactions, inverse Compton, and Bremsstrahlung, subject to losses) from the central -starburst- region of NGC 253. It is a multifrequency model, so that radio and IR data are also described. The resulting predictions for the very high energy regime (hundreds of GeV and TeV energies) are used to analyze whether one should expect NGC 253 to appear as a source for ground based Cherenkov telescopes.

1. Phenomenology of the central region of NGC 253

NGC 253 is located at a distance of ~ 2.5 Mpc and it is a nearly edge-on (inclination 78°) barred Sc galaxy. The continuum spectrum of NGC 253 has a luminosity of 4×10^{10} L$_\odot$ (Melo et al. 2002). The FIR luminosity is at least a factor of 2 larger than that of our own Galaxy, and it mainly comes from the central nucleus. IR emission can be understood as cold ($T \sim 50K$) dust reprocessing of stellar photon fields.

When observed at 1 pc resolution, at least 64 individual compact radio sources have been detected within the central 200 pc of the galaxy (Ulvestad & Antonucci 1997), and roughly 15 of them are within the central arcsec of the strongest radio source, considered to be either a buried active nucleus or a very compact SNR. Of the strongest 17 sources, about half have flat spectra and half have steep spectra. This indicates that perhaps half of the individual radio sources are dominated by thermal emission from H II regions, and half are optically thin synchrotron sources, presumably SNRs. There is no compelling evidence for any sort of variability in any of the compact sources over an 8 yr time baseline. The region surrounding the central 200 pc has also been observed with subarcsec resolution and 22 additional radio sources stronger than 0.4 mJy were detected within 2kpc of the galaxy nucleus (Ulvestad 2000). The region outside the central starburst may account for about 20% of the star formation of NGC 253. It is subject to a supernova explosion rate well below 0.1 yr^{-1}, and has an average gas density in the range 20–200 cm^{-3}, much less than the most active nuclear region (Ulvestad 2000).

Carilli (1996) presented low frequency radio continuum observations of the nucleus at high spatial resolution. Free-free absorption was claimed to be the mechanism producing a flattening of the synchrotron curve at low energies, with a turnover frequency located between $10^{8.5}$ and 10^9 Hz. The emission measures needed for this turnover to happen, for temperatures in the order of 10^4 K, is at least 10^5 pc cm^{-6}. As shown by infrared, millimeter, and centimeter observations, the 200 pc central region dominates the current star formation in NGC 253, and is considered as the starburst central nucleus (e.g., Ulvestad and Antonucci 1997, Ulvestad 2000). Centimeter imaging of this inner starburst, and the limits on variability of radio sources, indicates a supernova rate less than 0.3 yr^{-1} (Ulvestad & Antonucci 1997), which is consistent with results ranging from 0.1 to 0.3 yr^{-1} inferred from models of the infrared emission of the entire galaxy (Rieke et al. 1980; Rieke, Lebofsky & Walker 1988, Forbes et al. 1993). When compared with Local Group Galaxies, the supernova rate in NGC 253 is one order of magnitude larger (Pavlidou and Fields 2001).

Current estimates of the gas mass in the central 20" – 50" (< 600 pc) region range from 2.5 $\times 10^7$ M$_\odot$ (Harrison, Henkel & Russell 1999) to 4.8 $\times 10^8$ M$_\odot$ (Houghton et al. 1997), see Bradford et al. (2003), Sorai

et al. (2000), and Engelbracht et al. (1998) for discussions. For example, using the standard CO to gas mass conversion, the central molecular mass was estimated as 1.8×10^8 M$_\odot$ (Mauersberger et al. 1996). It would be factor of ~ 3 lower if such is the correction to the conversion factor in starburst regions which are better described as a filled intercloud medium, as in the case of ULIRGs, instead of a collection of separate large molecular clouds, see Solomon et al. (1997), Downes & Solomon (1998), and Bryant & Scoville (1999) for discussions. Thus we will assume in agreement with the mentioned measurements that within the central 200 pc, a disk of 70 pc height has $\sim 2 \times 10^7$ M$_\odot$ uniformly distributed, with a density of ~ 600 cm^{-3}. Additional target gas mass with an average density of ~ 50 cm^{-3} is assumed to populate the central kpc outside the innermost region, but subject to a smaller supernova explosion rate ~ 0.01 yr^{-1}, 10% of that found in the most powerful nucleus (Ulvestad 2000).

2. Diffuse modelling

The approach to compute the steady multiwavelength emission from NGC 253 follows that implemented in Q-DIFFUSE, which we have used with a few further improvements (Torres 2004). We refer the reader to Torres (2004) and Domingo-Santamaría & Torres (2005) for details. The steady state particle distribution is computed as the result of an injection distribution being subject to all losses and secondary production in the interstellar medium. The normalization of the spectrum is obtained from the total power transferred by supernovae into CRs kinetic energy within a given volume. For electrons, the total rate of energy loss considered is the sum of ionization, inverse Compton scattering, bremsstrahlung, adiabatic losses, and synchrotron radiation. For the production of secondary electrons, Q-DIFFUSE computes knock-on electrons and charged pion processes producing both electrons and positrons. In the case of γ-ray photons, we compute bremsstrahlung, inverse Compton and neutral pion decay processes. For radio photons, we compute, using the steady distribution of electrons, the synchrotron, and free-free emission. Free-free absorption is also considered in order to reproduce the radio data at low frequencies. The FIR emission is modelled with a dust emissivity law given by $\nu^\sigma B(\epsilon, T)$, where $\sigma = 1.5$ and B is the Planck function. The computed FIR photon density is used as a target for inverse Compton process as well as to give account of losses in the γ-ray scape. The latter basically comes from the opacity to $\gamma\gamma$ pair production with the photon field of the galaxy nucleus. The opacity to pair production from the interaction of a γ-ray photon in the presence of a nucleus of charge Z is considered too. For further details and relevant formulae see Domingo-Santamaría & Torres (2005).

3. Results

The numerical solution of the diffusion-loss equation for protons and electrons is shown in Figure 1a and 1b. We have adopted a diffusive residence timescale of 10 Myr, a convective timescale of 1 Myr, and a density of ~ 600 cm^{-3}. In the case of electrons, the magnetic field with which synchrotron losses are computed in Figure 1b is 300 μG. The latter is fixed requiring that the steady electron population produces a flux level of radio emission matching observations. An injection electron spectrum is considered –in addition to the secondaries– in generating the steady electron distribution. From about $E_e - m_e \sim 10^{-1}$ to 10 GeV, the secondary population of electrons dominates, in any case. The IR continuum emission is modelled with a spectrum having a dilute blackbody (graybody) emissivity law, proportional to $\nu^\sigma B(\epsilon, T)$, where B is the Planck function. Figure 1c shows the result of this modelling and its agreement with observational data when the dust emissivity index $\sigma = 1.5$ and the dust temperature $T_{\text{dust}} = 50K$. Whereas free-free emission is subdominant when compared with the synchrotron flux density, free-free absorption plays a key role at low frequencies, determining the opacity. We have found a reasonable agreement (see Figure 1d) with all observational data for a magnetic field in the innermost region of 300 μG, an ionized gas temperature of about 10^4 K, and an emission measure
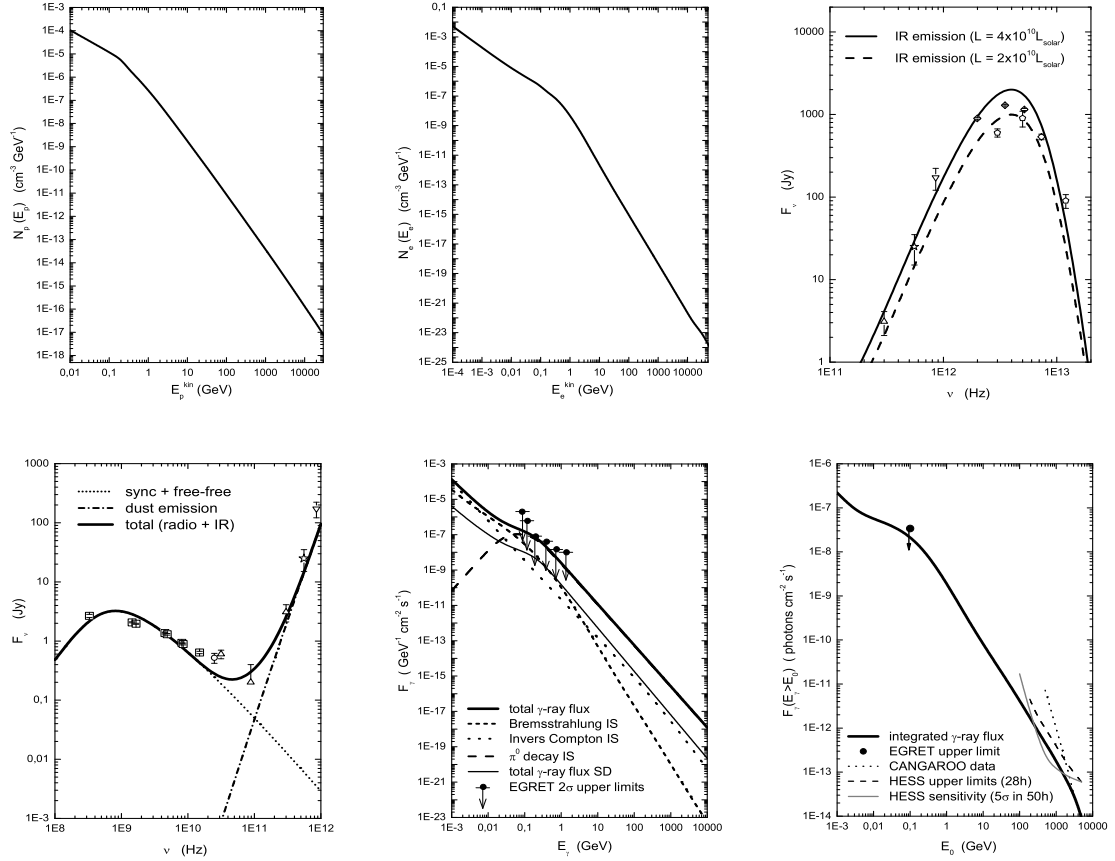
Figure 1. From top to bottom and left to right: a) Steady proton distributions in the innermost region of NGC 253. b) Idem for the steady electron distribution. c) IR flux from NGC 253 assuming a dilute blackbody with temperature $T_{\mathrm{dust}} = 50$ K and different total luminosities. d) Multifrequency spectrum of NGC 253 from radio to IR: comparison of experimental data points with the result of our modelling. e) Differential γ-ray fluxes from the central region of NGC 253. Total contribution of the surrounding disk is separately shown, as are the EGRET upper limits. Also shown are the relative contributions of bremsstrahlung, inverse Compton, and neutral pion decay to the γ-ray flux. f) Integral γ-ray fluxes. The EGRET upper limit (for energies above 100 MeV), the CANGAROO (Itoh et al. 2002) integral flux as estimated from their fit, the (4 telescopes) HESS sensitivity (for a 5σ detection in 50 hours), and the recently released (2 telescopes) HESS upper limit curve on NGC 253 (Aharonian et al. 2005) are given. Absorption effects are already taken into account.

of 5×10^5 pc cm^{-6}. Figure 1e shows bremsstrahlung, inverse Compton, and pion decay γ-ray fluxes from the central nucleus of NGC 253. These results are obtained with the model in agreement with radio and IR observations. Our predictions, while complying with EGRET upper limits, are barely below them. If this model is correct, NGC 253 is bound to be a bright γ-ray source for GLAST. The integral fluxes are shown in Figure 1f. Our model predicts that, given enough observation time, NGC 253 is also to appear as a point-like

source in an instrument like HESS.[1] Our fluxes are only a few percent of those reported by the CANGAROO collaboration. The effect of the opacity on the integral γ-ray fluxes only plays a role above 3 TeV.

4. Conclusions

The ease of all the assumptions made in our model, its concurrence with all observational constraints, and the unavoidability of the processes analyzed, lead us to conclude that 1) GLAST will detect NGC 253, being our predicted luminosity (2.3×10^{-8} photons cm^{-2} s^{-1} above 100 MeV) well above its 1 yr all sky survey sensitivity ; 2) that our predicted TeV fluxes are about one order of magnitude smaller than what was claimed to be detected by CANGAROO; and 3) that HESS should detect the galaxy as a point like source provided it is observed long enough ($\gtrsim 50$ hours, for a detection between 300 and 1000 GeV.)

5. Acknowledgements

References

[1] Aharonian F. A. et al. 2005, A&A, in press., astro-ph/0507370
[2] Bradford C. M., et al. 2003, ApJ 586, 891
[3] Bryant P. M., & Scoville N. Z. 1999, ApJ 117, 2632
[4] Carilli C. L. 1996, 305, 402
[5] Domingo-Santamaría E., & Torres D.F. 2005, astro-ph/0506240
[6] Downes D., & Solomon P.M. 1998, ApJ 507, 615
[7] Engelbracht C. W., Rieke M. J., Rieke G. H., Kelly D. M. & Achterman J. M. 1998, ApJ 505, 639
[8] Forbes D.A., et al. 1993, ApJ 406, L11
[9] Harrison A., Henkel C. & Russel A. 1999, MNRAS 303, 157
[10] Houghton S., et al 1997, A&A 325, 923
[11] Itoh C., et al. 2002, A&A 396, L1
[12] Mauersberger R., Henkel C., Wiebelinski R., Wiklind T. & Reuter H.-P. 1996, A&A 305, 421
[13] Melo V. P., et al. 2002, ApJ 574, 709
[14] Pavlidou, V., & Fields, B. 2001, ApJ, 558, 63
[15] Rieke G. H., Lebofsky M. J., Thompson R. I., Low F. J. & Tokunga A. T. 1980, Ap. J. 238, 24
[16] Rieke G. H., Lebofsky M. J. & Walker C. E. 1988, ApJ 325, 679
[17] Solomon P. M., Downes, D., Radford, S. J. E. & Barrett, J.W. 1997, ApJ, 478, 144
[18] Sorai K., Nakai N., Nishiyama K. & Hasegawa T. 2000, Publ. Astron. Soc. Japan 52, 785
[19] Torres, D. F. 2004, ApJ 617, 966
[20] Ulvestad J. S. 2000, ApJ 120, 278
[21] Ulvestad J. S. & Antonucci R. R. J. 1997, ApJ 488, 621

---

[1] The HESS array has just released (Aharonian et al. 2005) their results for NGC 253, based on a total of 28 hours taken during the construction of the array with 2 and 3 telescopes operating. The energy threshold for this dataset was 190 GeV. Upper limits from HESS on the integral (99 % confidence level) are shown in Figure 1f. As an example, above 300 GeV, the upper limit is 1.9×10^{-12} photons cm^{-2} s^{-1}. Our predictions are below these upper limits at all energies but still above HESS sensitivity for reasonable observation times.